Research Article

# Synthesis of bio-degradable poly(2-hydroxyethyl methacrylate) using natural deep eutectic solvents for sustainable cancer drug delivery

Periyakaruppan Pradeepkumar[1] · Anbalagan Subbiah[2] · Mariappan Rajan[1]



**Abstract**

The primary metabolites frequently used for various applications including medicinal applications. Currently, natural deep eutectic solvents (NADESs) is prepared through primary metabolites and it is a good solvent with better biocompatibility, biodegradability, and non-toxic nature. In the current study, NADES was designed and used for the polymerization to drug carrier synthesis. The maximum quantity of poly(HEMA) was obtained by the stoichiometric ratios of choline chloride and xylitol (1:1) of NADES. The NADES-poly(HEMA) was attempted as a carrier with loaded 5-fluorouracil (5-FU). The NADES formation and PHEMA were characterized by proton nuclear magnetic resonance ($^1$H NMR), Fourier-transform infrared spectroscopy. The phase purity of synthesised NADES-poly(HEMA) and 5-FU loaded NADES-poly(HEMA) carrier was investigated by X-ray diffraction. Furthermore, the scanning electron microscope exhibited as-synthesised NADES-poly(HEMA) and 5-FU loaded NADES-poly(HEMA) was smooth with interconnected porous morphology. The encapsulation efficiency of the carrier was obtained 77 ± 1% and in vitro of 5-FU release from NADES-poly(HEMA) carrier was achieved in various physiological environment. Biodegradability of NADES-poly(HEMA) carrier was determined in the presence of esterase enzyme. The enhanced cytotoxicity of 5-FU-loaded NADES-poly(HEMA) was investigated against HeLa cancer cell line. Thus, the newly developed 5-FU loaded NADES-poly(HEMA) carrier is suitable for cancer treatment over a prolonged period of drug release.

**Electronic supplementary material** The online version of this article (https://doi.org/10.1007/s42452-019-0591-4) contains supplementary material, which is available to authorized users.

✉ Mariappan Rajan, rajanm153@gmail.com | [1]Biomaterials in Medicinal Chemistry Laboratory, Department of Natural Products Chemistry, School of Chemistry, Madurai Kamaraj University, Madurai, Tamil Nadu 625021, India. [2]R&D Centre, Bal Pharma LTD, Bangalore, Karnataka 560099, India.

SN Applied Sciences (2019) 1:568 | https://doi.org/10.1007/s42452-019-0591-4

Received: 2 March 2019 / Accepted: 9 May 2019 / Published online: 15 May 2019

**Graphical abstract**

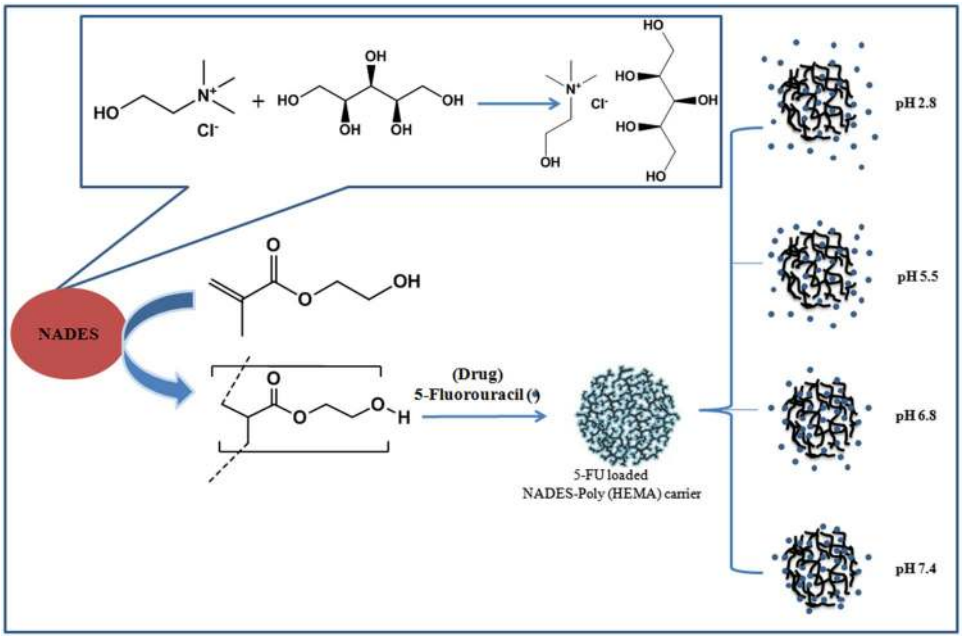


**Keywords** Drug delivery · 2-Hydroxyethyl methacrylate · Natural deep eutectic solvent · Polymerization

## 1 Introduction

Deep eutectic solvents (DESs) is a great potential usage for biomedical applications including organic reaction, electrochemical reaction, nanoparticles synthesis, enzyme catalyst, and polymerization reactions, etc. [1–3]. The development of deep eutectic solvents was prepared by using primary metabolites and secondary metabolites which is called natural deep eutectic solvents (NADESs). The NADESs had attracted much more attention due to the increasing solubility of the different compounds such as carbohydrates, synthetic polymers, and metal chloride etc., and also it have promising alternative to organic solvents [4, 5]. NADESs is less expensive, non-toxic, sustainable, biodegradable, and biocompatible because NADESs is a combination of naturally available metabolites [6–12]. The NADESs was prepared by the endothermic complexation of hydrogen bond donor (HBD) for examples citric acid/xylitol/sucrose/tartaric acid/ethylene glycol/malonic acid/malic acid and hydrogen bond acceptor (HBA) such as Choline Chloride, *N*-ethyl-2-hydroxy-*N*,*N*-dimethylethanaminium chloride/*N*-benzyl-2-hydroxyl-*N*,*N*-dimethylethanaminium/methyltriphenylphosphonium bromide/*N*,*N*-diethyl ethanol ammonium chloride molecules were formed by self- association via hydrogen bonds [13]. In these, hydrogen bond formations for charge delocalization between halide anion and the hydrogen donor moiety is the responsible for the decreasing in the freezing point of the mixture relative to the melting points of its individual compounds [14].

NADES have been used as active pharmaceutical ingredients (API) [15] in the pharmaceutical industry. The API-NADES compounds offer improved properties, such as increased stability, solubility, permeability and drug delivery than comparable solid pharmaceutical forms [16]. poly(octane diol-*co*-citrate)-lidocaine was developed as DESs for local anesthetic drug delivery [17]. The system has reported rapid drug releasing properties with the non-specific drug releases. Meanwhile, increasing the prolonged releases and reducing the side effects, the researchers were concentrated polymeric drug carrier. In view of shortcomings, Methacrylate and its derivatives was frequently used preparation of biomaterials for drug release [18, 19]. The individuality that made for the polymer potential materials for biological applications such minimal inflammatory reaction with tissues, greater fracture resistance, good solubility, biodegradation, excellent biocompatibility, and sustained drug release. Methacrylate and its derivatives was widen application with combination of other polymers like chitosan [20], polyurethane [21], gelatin [22] etc. A previous research, methacrylate derivative was prepared by using a different organic

solvent which is highly toxic nature, it has been not suitable for drug delivery applications [23].

The anticancer drug delivery system was limited to develop using NADES with a combination of another polymer [16, 24–27]. In this present study, the feasibility of the formation of HEMA polymerization of the biodegradable system was demonstrated with a new combination of natural deep eutectic solvents. The ability of drug loading and release properties were investigated with different physiological conditions and cytotoxicity effect with cellular uptake, and apoptosis was studied on HeLa cancer cell line.

## 2 Materials and method

### 2.1 Materials

Choline chloride, xylitol was obtained from Himedia, India. 2-Hydroxyethyl methacrylate (HEMA) and 5-Fluorouracil (5-FU) were obtained from Sigma-Aldrich, India. Chloroform, diethyl ether, ethyl acetate, acetone were purchased from Merck, India. All other chemicals are analytical grade and it was used without further purifications. Double distilled water was used for all experimental procedures.

### 2.2 Preparation of natural deep eutectic solvents (NADESs)

NADES was prepared by a previously described method with slight modifications [28]. In brief, hydrogen bond acceptor (HBA) salt of choline chloride and hydrogen bond donor (HBD) salt of xylitol were mixed in a round bottom flask and warmed at 37 °C with constant blending with different molar proportion (1:1; 1:2; 1:3; and 2:1) under $N_2$ atm until homogeneous fluids were formed (S. Fig. 1). The homogenous liquid collected; purified and formed the structure of the NADESs was investigated by using $^1$H-NMR spectroscopy.

### 2.3 Polymerization of 2-hydroxyethyl methacrylate

NADES-poly(HEMA) was prepared by a slight modified of a previously reported procedure [16]. Briefly, 1 ml (0.0034 mol) of NADES (1:1) and 0.4 ml (0.44 mol) of HEMA were taken in a 50 ml of round bottom flask, and the reaction mixture was stirred with constant stirring at room temperature (50 °C) for 2 h and then allowed to polymerize up to 24 h at 70 °C. The obtained polymer product was collected and cooled to room temperature (37 °C). After polymer product, ethanol was added to remove the unreacted reactants. The purified polymer was used for further characterizations [29].

### 2.4 Drug loaded NADES-poly(HEMA)

The carrier (100 mg) was placed in a 20 ml beaker. 5-Fu in ethanol (50 mg/ml) was added on the carrier and stirred for 1 h. The supernatant solution from the 5-Fu loaded carrier mixture solution was removed at 15 min intervals and analyzed by UV spectrometer (Shimadzu-UV 1600) at a $\lambda_{max}$ 280 nm [30].

$$\text{Encapsulation efficiency } (\%) = \frac{\text{Total amount of drug} - \text{Free amount of drug}}{\text{Total amount of drug}} \times 100 \quad (1)$$

### 2.5 In vitro release study

The in vitro drug releases were analyzed by using a dialysis membrane technique [31]. 5-FU releases from 5-FU loaded NADES-poly(HEMA) carrier were assessed as follows: 10 mg of 5-FU-loaded NADES-poly(HEMA) was added to the buffer solution (5 ml; pH 2.8, 5.5, 6.8, and 7.4) in the dialysis membrane bag at 27 °C and it was placed in a dialysis membrane. The dialysis membrane was incubated in a 50 ml water containing beaker at 27 °C with constant stirring at 100 rpm. At 10 min time intervals, 2 ml of the sample solution was taken and an equal amount of freshly make pH solution was added to maintain the equal volume of the system. The 5- FU cumulative release was measured using a UV spectrometer (Shimadzu-1600) at the $\lambda_{max}$ 267 nm.

### 2.6 In vitro enzymatic degradation and weight loss analysis

In vitro bio-degradation property of the NADES-poly(HEMA) carrier was investigated in different pH solutions (2.8 and 6.8) with esterase enzyme at the concentration of 0.2 mg/ml. The biodegradation of NADES-poly(HEMA) carrier was carried out in a small vial containing 10 mg of the sample and 10 ml of pH solution with esterase enzyme. The vial was incubated with esterase for enzymatic activity at 27 °C with a constant stirring (100 rpm). At predetermined immersion duration, 5-FU loaded NADES-poly(HEMA) carrier sample were removed from the incubation medium and washed gently with distilled water. The NADES-poly(HEMA) carrier was lyophilized at − 40 °C in a lyophilizer (Sub Zero Lyophilizer, Chennai, India) and determined weight loss. The weight loss of the 5-FU loaded NADES-poly(HEMA) was estimated based on the following Eq. (2).

$$\text{Degradation } (\%) = \frac{W0 - Wt}{W0} \times 100 \quad (2)$$

where W0 is the original dry mass of NADES-poly(HEMA), Wt is the residual dry mass of NADES-poly(HEMA) after degradation with different time periods.

## 2.7 Physicochemical characterizations

### 2.7.1 Density

The densities of the prepared (ChoCl:Xylitol) mixtures were obtained using specific gravity bottle with a standard accuracy of ± 14.01 g $cm^{-3}$. The estimated uncertainty of the density measurements was observed ± 2 g $cm^{-3}$.

### 2.7.2 Nuclear magnetic resonance spectroscopy technique

NMR spectra were recorded in (Bruker 300 $MH_Z$) instrument with tetramethylsilane as an internal standard, and using $CDCl_3$ as the solvent. Chemical shifts are given in parts per million (ppm).

### 2.7.3 Fourier transforms infrared spectroscopy analysis

The confirmation of the functional changes of NADES, poly(HEMA) polymerization and 5-FU loaded NADES-poly(HEMA) carrier formation was analyzed by FT-IR spectroscopy (Spectrum GX-I, Perkin Elmer, Waltham, MA, USA). The transmission scanning mode in the spectral area was 4000–1000 $cm^{-1}$ and KBr pellets used for the sample preparation.

### 2.7.4 X-ray powder diffraction (XRD) analysis

XRD (PW3040/60 X-pert PRO, Almelo, Netherlands) was used to characterize using analysis of phase identification of NADES-poly(HEMA) carrier and 5-FU loaded NADES poly(HEMA) carrier.

### 2.7.5 TGA analysis

The thermal stability of the NADES-poly(HEMA) carrier and 5-FU loaded NADES poly(HEMA) carrier was assessed by the thermogravimetric instrument (SDTQ-600) in the $N_2$ atmosphere at a scanning rate of 10 K/min from 25 to 800 °C.

### 2.7.6 Scanning electron microscope (SEM) analysis

The surface morphology of the NADES-poly(HEMA) carrier and 5-FU loaded NADES-poly(HEMA) carrier were analyzed by using SEM (JEOL JSM LV-5600). Dispersion of the NADES-poly(HEMA) carrier and 5-FU loaded NADES-poly(HEMA) carrier drop was placed onto a glass plate and dried at 27 °C. The plate was mounted on a plate using double side carbon adhesive tab and was then coated with gold using an ion sputter. The coating was attained at 25 mA for the 60 s. Scanning was performed under high vacuum and room temperature, with a beam voltage of 20–30 kV.

## 2.8 Biological characterizations

### 2.8.1 Cell culture maintenance

A human cervical cancer cell line (HeLa cell) was purchased from the National Centre for Cell Science (Pune, India) and cultured for in vitro experiments studies. For culturing minimal essential medium supplemented with 13% heal inactivated FBS, penicillin/streptomycin grown at 37 °C was used 5% $CO_2$ in air atmosphere.

### 2.8.2 In vitro cytotoxicity of 5-FU loaded NADES-poly(HEMA)

The anticancer efficiency of 5-FU loaded NADES-poly(HEMA) carrier was investigated on HeLa cancer cell line. Pure cell line and NADES-poly(HEMA) carrier as a control groups and 5-FU loaded NADES-poly(HEMA) carrier was studied cytotoxicity efficacy by MTT (3-(4,5-dimethylthiazol-2-yl)-2,5-diphenyltetrazolium bromide) assay method [32]. HeLa cancer cell line was seeded in 96-well plates at a density of $1 \times 10^5$ cells per well plate and incubated with the samples for 24 h at 37 °C in an atmosphere of 5% $CO_2$. Different concentrations such as 50, 75, and 100 µg of 5-FU loaded NADES-poly(HEMA) carrier were added to each well and cultured for a further 1, 7 and 14 days. Then, of MTT (3-(4,5-dimethylthiazol-2-yl)-2,5-diphenyltetrazolium bromide) assay solution (50 µl) was added to each cell well and incubated at 37 °C. The medium containing unreacted MTT was completely removed by PBS solution carefully and measured the intensity at an absorbance–wavelength of 570 nm in the UV–visible spectrometer. The cell viability was compared with control cells.

### 2.8.3 Cellular uptake studies

5-FU loaded NADES-poly(HEMA) carrier were suspended in a cell culture medium at the concentration of 100 µg/ml. HeLa cells were a culture in 96 well plates for 24 h. Moreover, control was also performed above the culture medium. After incubation of 24 h, the culture medium was removed and cells were washed two times with PBS solution. Cells were stained with 30 min incubation with a 0.25% solution of DAPI and 0.2% of Tublin in PBS with 1% of Bovine Serum Albumin [33]. This was done to visualize the cell nucleus (blue) and cell membrane (red) by

confocal microscope (Olympus IX 81 under DU897 mode, Tokyo, Japan).

## 3 Results and discussion

### 3.1 Preparation of natural deep eutectic solvents

Natural deep eutectic solvents were prepared through simple blending method at 37 °C. The desired amount of the choline chloride was mixed with a stoichiometric ratio of the hydrogen bond donor of xylitol molecule. Both compounds were mixed thoroughly with a different ratio like 1:1; 1:2; 1:3 and 2:1 at 37 °C. The ratio increases from 1:1 to 1:3 the viscosity gradually decreases and in the case of 2:1 form as solid, when the mixing of both compounds. The 1:1 ratio of NADES was the transparent liquid and it is used for reactions. The clear NADES solution was offered for synthesis and polymerization reaction to make and control the drug delivery system [34, 35]. The density of the solvent is very important for chemical reactions, extraction and solubility of the compounds. The use of transparent NADES favored the easy tuning of the ratio of hydrogen bond donating compounds to a certain threshold value those NADESs [36]. The formation of the NADES was initially confirmed by the homogeneous liquid and it further characterized.

The compositions of the four different ratios of the NADES solvent physicochemical properties were listed in the Table 1. The obtained NADES solvent is well correlated with the system of ChoCl + urea based DES [37]. The highest density was recorded for 1:1 of NADES, which showed a maximum of 1.5 g $cm^{-3}$ at 27 °C whereas the ratio of 1:2, 1:3, and 2:1 showed the lowest densities 1.1 g $cm^{-3}$, 1 g $cm^{-3}$, and 1.3 g $cm^{-3}$ of the measurement of at 27 °C. The present results showed that the increase molar ratio of hydrogen donor in the mixture, which is expected due to the clear role that the hydrogen bond strength between the molecules decreases, because decreased in the densities. The experimental densities were calculated by the Eq. (3):

**Table 1** Optimization reaction with different molar ratio for the polymerization of HEMA ChoCl:Xylitol (1:1) and density value

| S. no. | NADES | Molar ratio | Tem (°C) | Density (g $cm^{-3}$) | Observation |
|---|---|---|---|---|---|
| 1 | ChoCl:Xylitol | 1:1 | 27 | 1.5 | Transparent liquid |
| 2 | ChoCl:Xylitol | 1:2 | 27 | 1.1 | Semi solid |
| 3 | ChoCl:Xylitol | 1:3 | 27 | 1.0 | Semi solid |
| 4 | ChoCl:Xylitol | 2:1 | 27 | 1.3 | Solid |

$$\rho = \frac{m}{V} \quad (3)$$

where ρ (g $cm^{-3}$) is the density; m is the mass of bottle; v is the volume of the substance. The 1:1 ratio of NADES solvent used for the polymerization process and the scheme for the NADES-poly(HEMA) formation is represented as in Scheme 1.

### 3.2 NMR spectroscopy analysis

The formation of ChoCl:Xylitol based NADES was characterized by using $^{1}$H-NMR technique for the determination of structure of the formed solvent and results were presented in S. Fig. 2. The HBA compound of ChoCl characteristic signal of the proton values of 4.10 ppm for (OH–C**H**$_2$–$CH_2$–N–$(CH_3)_3$), 3.56 ppm for (OH–$CH_2$–C**H**$_2$–N–$(CH_3)_3$) and 3.55 ppm for (OH–$CH_2$–$CH_2$–N–(C**H**$_3$)$_3$) appeared and presented in S. Fig. 2A. The HBD compound of Xylitol showed proton signals from 3.35 ppm for ($OHCH_2$–OHCH–OHC**H**–OHCH–$CH_2OH$), 3.42 ppm for ($OHCH_2$–OHC**H**–OHCH–OHCH–$CH_2OH$), 3.55 ppm for ($OHCH_2$–O**H**CH–O**H**CH–O**H**CH–$CH_2OH$), 4.13 ppm for (O**H**$CH_2$–OHCH–OHCH–OHCH–$CH_2$O**H**), and 4.50 ppm for (OHC**H**$_2$–OHCH–OHCH–OHCH–C**H**$_2$OH) (S. Fig. 2B.). The formed ChoCl:Xylitol (NADES) showed proton signals of 3.3 ppm for ($OHCH_2$–$CH_2$–N(C**H**$_3$)$_3$), 3.89 ppm for (OH–$CH_2$–C**H**$_2$–$N(CH_3)_3$), 3.62 (OH–C**H**$_2$–$CH_2$–$N(CH_3)_3$), 3.53 ppm for (OHC**H**$_2$–OHCH–OHCH–OHCH–C**H**$_2$OH–xylitol), 3.48 ppm for ($OHCH_2$–OHC**H**–OHCH–OHC**H**–$CH_2$OH–xylitol), 3.34 ppm for ($OHCH_2$–OHCH–OHC**H**–OHCH–$CH_2$OH–xylitol), 3.57 ppm for (OH···Cl). From the spectrum, the hydrogen bonding of (OH···Cl) group is obvious demonstrating the interaction of ChoCl and Xylitol solvent to form NADES (S. Fig. 2C). The characteristic signal of NADES protons was shifted to downfield compared to free ChoCl and Xylitol protons. Downfield chemical shifts were indicative of the formation of hydrogen bond formation [38]. The excess hydroxyl group of NADES did not appear in a spectrum. This can be done by the rapid exchange of NADES proton with $D_2O$ solvent [39].

### 3.3 FT-IR analysis

The FT-IR spectrum of HEMA, poly(HEMA) and 5-FU loaded NADES-poly(HEMA) was presented in Fig. 1. Figure 1a shows the typical spectra of HEMA; the characteristic peaks at 1295, 1640 1724, and 3415 $cm^{-1}$ in a response to the presence of C–H, C=C, C=O, and OH groups respectively. In Fig. 1b shows that the characteristic peaks of poly(HEMA) and the peaks corresponds to the formation of a polymer from monomers such as 1295–1301, 1640–1645,

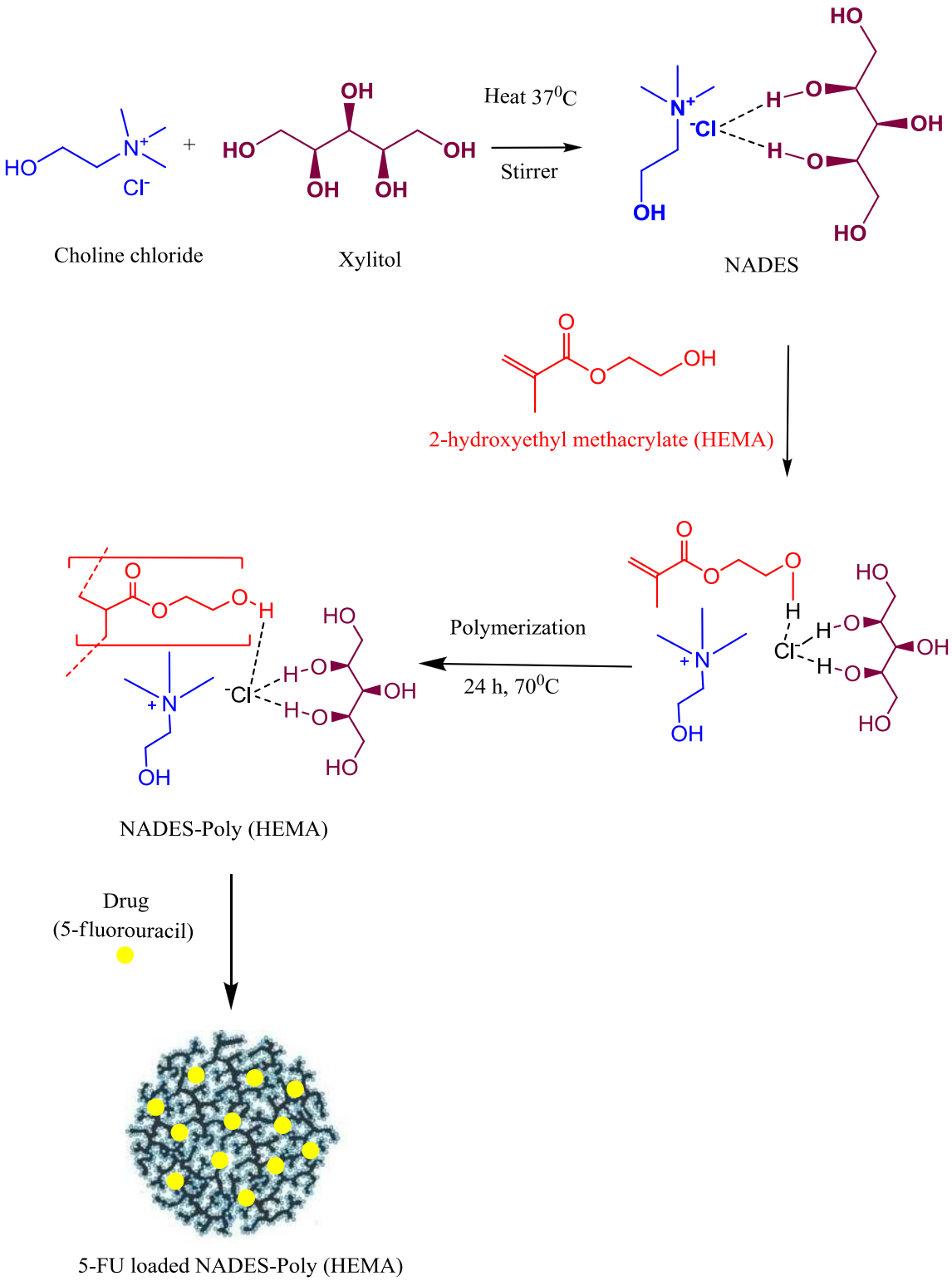


**Scheme 1** Synthetic pathway for the formation of 5-FU loaded NADES-poly(HEMA) carrier

and 1724–1708 $cm^{-1}$. The major significant polymer peak is observed from 3415–3423 $cm^{-1}$. This peak corresponding to hydroxyl groups (–OH) showed broad peak and high intensity compared with HEMA hydroxyl peak. It indicates that hydroxyl was hydrogen bonded with NADES and it forms as NADES-poly(HEMA) carrier. Moreover, the overall

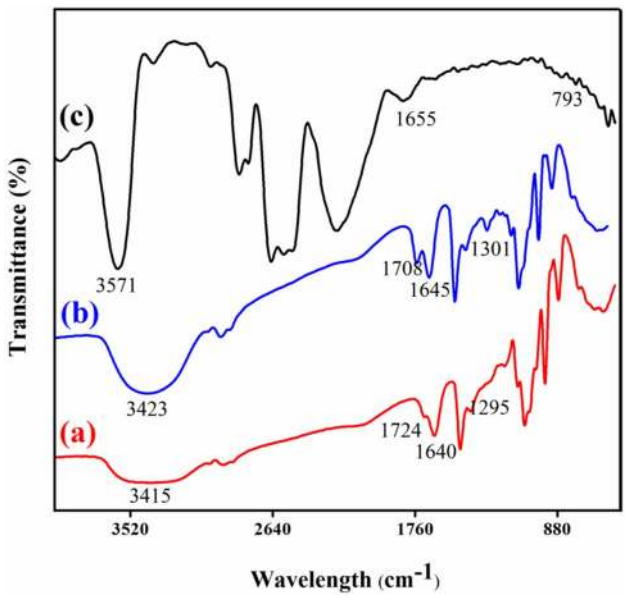


**Fig. 1** FT-IR spectrum of (a) NADES-Mono (HEMA), (b) NADES-poly(HEMA), and (c) 5-FU loaded NADES-poly(HEMA) carrier

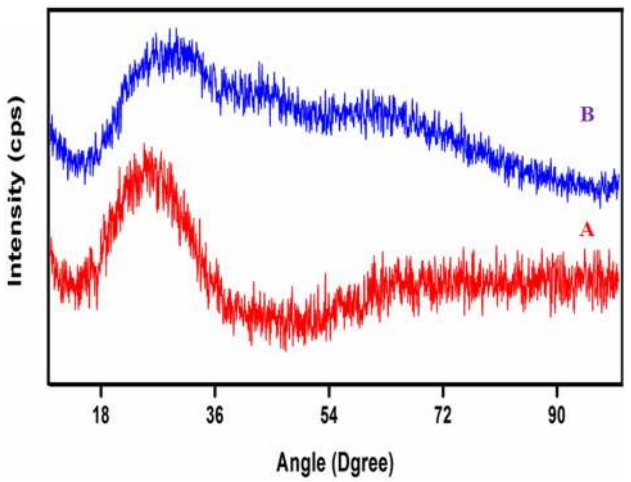


**Fig. 2** XRD pattern of (a) NADES-poly(HEMA) carrier and (b) 5-FU loaded NADES-poly(HEMA) carrier

polymer peaks were shifted from the monomer peaks. These shifted peaks might be ascribed to the polymer formation [16]. The FT-IR spectrum of 5-FU loaded NADES-poly(HEMA) shows the characteristic peaks at 3571 $cm^{-1}$ corresponded to the N–H stretching vibration, other characteristic peaks indicates the C=O stretching vibration at 1655 $cm^{-1}$ and the spectrum of C–F peaks stretching vibrations observed at 793 $cm^{-1}$ of the 5-FU (Fig. 1c). The peaks at 793 $cm^{-1}$(C–F) demonstrated the encapsulation of 5-FU drug loaded on the NADES-poly(HEMA) carrier.

### 3.4 XRD analysis

The XRD patterns of NADES-poly(HEMA) carrier and 5-FU loaded NADES-poly(HEMA) carrier were shown in Fig. 2. Form the XRD analysis, a broad peak at the 2θ value of around 25° appears, and it indicates the semi-crystalline nature of NADES-poly(HEMA) carrier. After 5-FU loaded on NADES-poly(HEMA), attributed peak shifted to 2θ value of 29° and the intensity was reduced significantly compared with an unloaded carrier (Fig. 2b). This is due to the encapsulation of 5-FU on the carrier reduce the crystalline nature of the carrier. The amorphous nature is significantly involved in the drug delivery [40] and also two new peaks are noticeable at the 2θ value of 44.39°, 64.64°. This indicates that the drug loaded on the carrier has good interaction and forms amorphous formulation. These were confirmed, the successful loading of the 5-FU drug on NADES-poly(HEMA) carrier and change of phases with the interaction of drug and the carrier.

### 3.5 TGA analysis

The decomposition and thermal stability of the NADES-poly(HEMA) and 5-FU loaded NADES-poly(HEMA) carrier were analyzed by TGA, which is shown in Fig. 3. Figure 3a shows the thermal and decomposition of the NADES-poly(HEMA) over a four-stage degradation process, the first stage is a 130–255 °C related to the evaporation of the moisture, absorbed water molecule on the NADES-poly(HEMA) and weight loss occurred > 15%. The second stage from 290 to 320 °C corresponds to the elimination of strong hydrogen bond interaction between choline chloride and xylitol, $CO_2$, CO and weight loss was observed at > 26% [41, 42]. The third weight loss from 410 to 470 °C

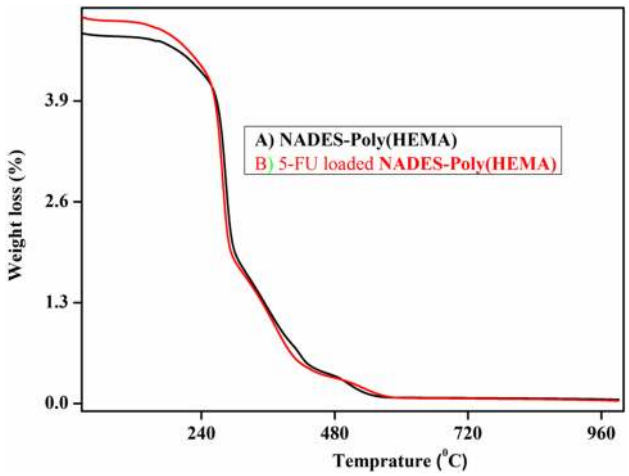


**Fig. 3** TGA measurements for (a) NADES-poly(HEMA) carrier and (b) 5-FU loaded NADES-poly(HEMA) carrier

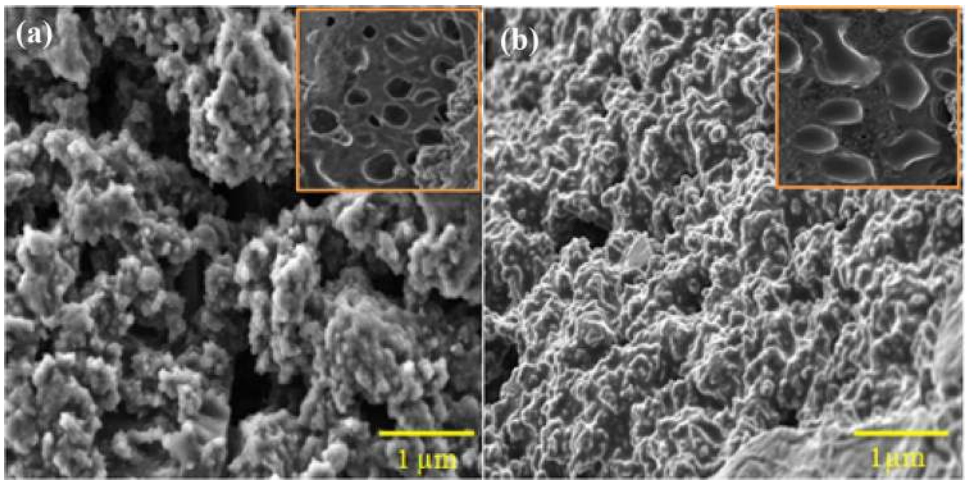


**Fig. 4** SEM images of **a** NADES-poly(HEMA) carrier, **b** 5-FU loaded NADES-poly(HEMA) carrier

was related to the decomposition of poly(HEMA) interacted NADES and weight loss occurred at > 16%; final weight loss from 510 to 570 °C associated with the aliphatic chains of poly(HEMA). After the loading of 5-FU, the degradation process was slightly increased due to the 5-FU molecules being located in the carrier, which shows excellent thermal stability when compared to the poly(HEMA) (Fig. 3b). From these results, the higher thermal stability of the carrier is suitable for anticancer drug delivery application due to the heat induced release stability of chemotherapeutic applications.

### 3.6 SEM analysis

The surface morphology of the NADES-poly(HEMA) carrier and 5-FU loaded NADES-poly(HEMA) carrier are given in Fig. 4a, b. From Fig. 4a, it can be noted uniform and interconnected porous nature of NADES-poly(HEMA) carrier. The porous of NADES-poly(HEMA) carrier is obliging for drug loading and it is significant role in the drug delivery applications. The 5-FU loaded NADES-poly(HEMA) carrier shows that the drugs were adsorbed (entrapped) and filled (encapsulated) in the porous of the carrier. The drug loaded 5-FU on NADES-poly(HEMA) was clearly shown in the SEM image (inner image of Fig. 4a, b). The porous structure provided a high surface area as well as a large number of surface functionalities of NADES-poly(HEMA) carrier, supporting the drug molecules binding to as physical interactions.

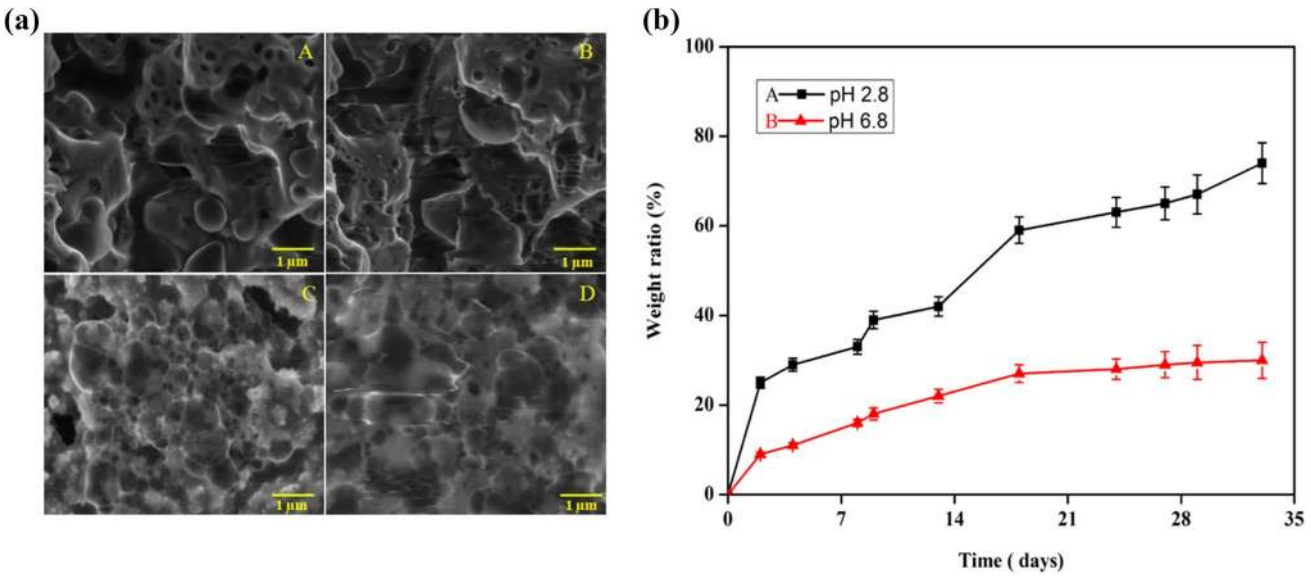


**Fig. 5** **a** SEM images of NADES-poly(HEMA) carrier in 0.2 mg/ml (esterase enzyme) and pH 2.8 solution. **A** Control for 0 day, **B** 10 day, **C** 20 day, and **D** 30 day; **b** the degradation study of 5-FU loaded poly(HEMA) carrier at pH 2.8 and 6.8

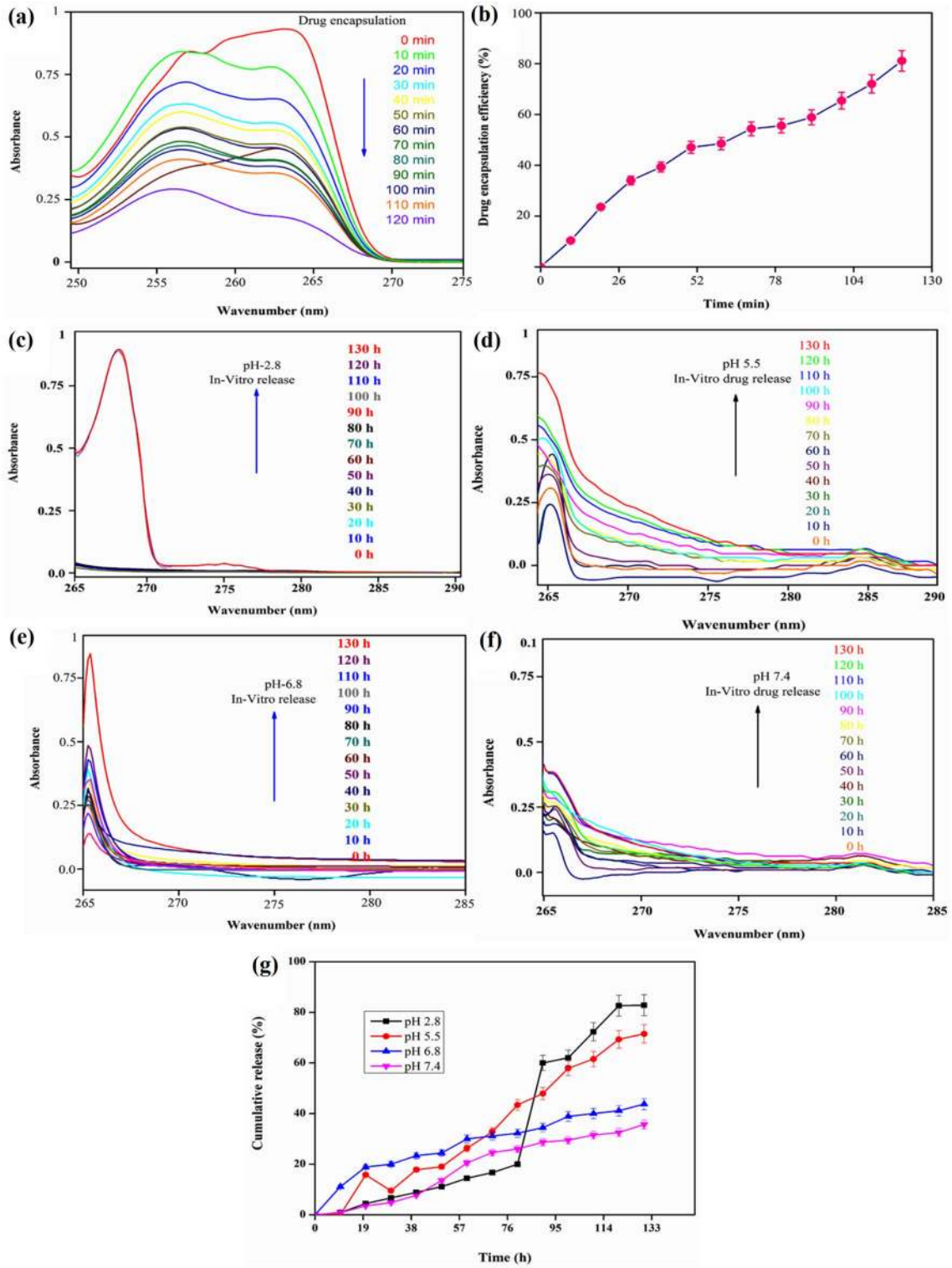


**Fig. 6** **a** Drug encapsulation efficiency of NADES-poly(HEMA) carrier and **b** in vitro release profile of 5-FU loaded NADES-poly(HEMA) carrier at **c** pH 2.8, **d** 5.5, **e** 6.8, **f** 7.4, **g** cumulative drug release pattern of 5-FU loaded NADES-poly(HEMA) carrier

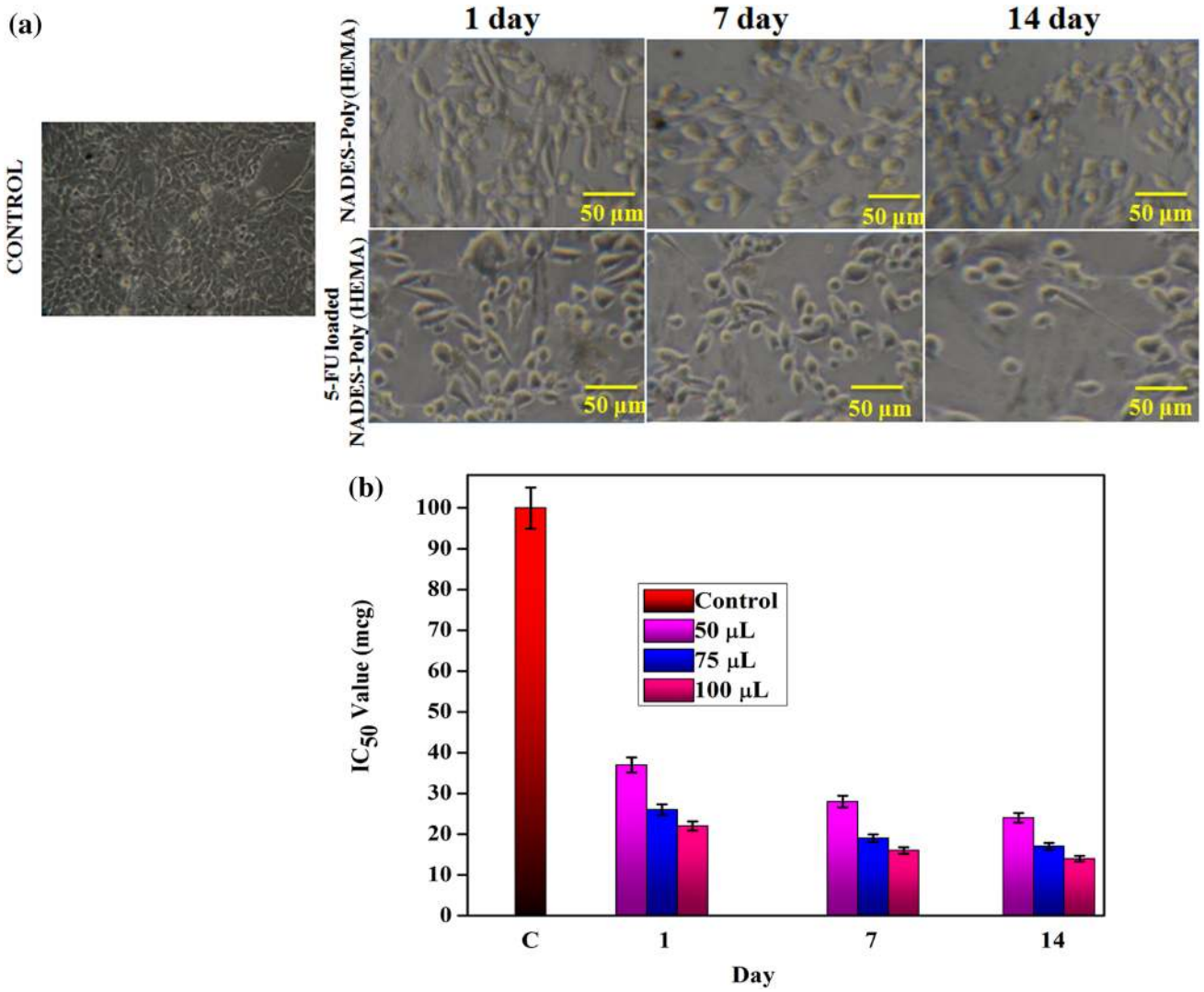


**Fig. 7** **a** Cytotoxicity effect of NADES-poly(HEMA) carrier and 5-FU loaded NADES-poly(HEMA) carrier treated on HeLa cell line. **b** $IC_{50}$ values of control is a (pure cell), different days (1, 7, and 14 days) and concentrations of 5-FU loaded NADES-poly(HEMA) samples 50 µg, 75 µg, and 100 µg used to treat with HeLa cell

### 3.7 Biodegradation and weight losses analysis

The degradation property of the NADES-poly(HEMA) carrier was investigated in different pH solutions (pH 2.8 and 6.8) with esterase enzyme at room temperature (27 °C), which is depicted in Fig. 5. The ester bonds of NADES-poly(HEMA) carrier are readily hydrolyzed broken with esterase enzyme. The biodegradability of NADES-poly(HEMA) carrier was estimated the weight loss and the morphological changes were captured through SEM technique (Fig. 5a). The biodegradation rates of NADES-poly(HEMA) carrier were shown in Fig. 5b. From this figure, the biodegradability rate was increased with increasing with incubation time. After 30 days of incubation period, the NADES-poly(HEMA) carrier morphological structure was totally changed with an irregular breakup. The NADES-poly(HEMA) carrier had 72 ± 1% of weight loss (pH 2.8) when compared with the zero day of incubation with enzyme. In contrast with, the drug-loaded carrier has a 32 ± 1% weight loss (pH 6.8) in compared with 0 days without enzyme. This result strongly suggests that carrier has biodegradability and biocompatible nature in pH 2.8 condition.

### 3.8 Encapsulation efficiency and in vitro drug release

The encapsulation efficiency of NADES-poly(HEMA) carrier has been investigated by UV–visible Spectroscopy and the results is shown in Fig. 6a. Encapsulation efficiency of 5-FU

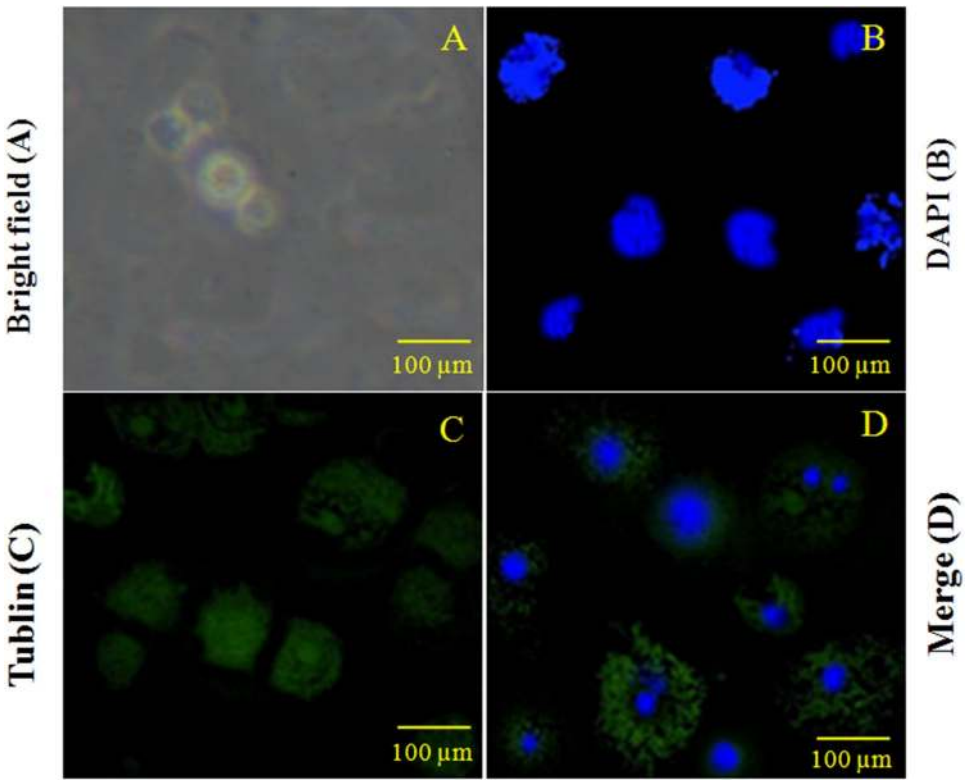


**Fig. 8** Confocal laser scanning microscopy images of HeLa cell incubated with 5-FU loaded NADES-poly(HEMA) carrier for 24 h. **a** Bright filed (HeLa cell line), **b** DAPI-stained HeLa cells (blue), **c** 5-FU encapsulated NADES-poly(HEMA) carrier loaded tubulin are red colour, and **d** the merged image was the overlapping image obtained by DAPI (blue) and nucleus (red)

on NADES-poly(HEMA) carrier increased with time due to the interactions between drug and carrier. The encapsulation of drugs is depends upon the solubility of drug in the NADES-poly(HEMA) medium [43]. It was achieved 77% of encapsulation efficiency. After loaded 5-FU loaded NADES-poly(HEMA) carrier was investigated the releasing properties of 5-FU from the carrier. The in vitro drug releasing profile of 5-FU loaded carrier was investigated in the pH 2.8, 5.5, 6.8, and 7.4; it was presented in Fig. 6g. The drug release at pH 5.5, 6.8, and 7.4 the 5-FU was then slowly released from the carrier up to 73.0%, 43%, and 33% of 5-FU in 130 h. At the same time period, 5-FU release was obtained 85.0% at the pH 2.8 solution. The releasing rate of 5-FU from NADES-poly(HEMA) carrier was higher in pH 2.8 medium compared with pH 5.5, 6.8, and 7.4 medium. The degradation of the carrier is one the main factors in drug release mechanism and in acidic environment the carrier ester bond easily broken compared with the neutral condition [44]. This clearly says that NADES-poly(HEMA) carrier is pH sensitive and the drug released as a controlled manner.

### 3.9 Cytotoxicity studies

The cell viability and cytotoxicity activity of the NADES-poly(HEMA) carrier and 5-FU loaded NADES-poly(HEMA) carrier was analyzed by MTT assay method and results was represented in Fig. 7. From this Fig. 7a, Days-dependent cell viability and cytotoxicity was observed in free carrier and 5-FU loaded carrier. The inhibitory concentration value [$IC_{50}$—39.07 µg] of the two samples is shown in (Fig. 7b). The treatment of HeLa cell line with NADES-poly(HEMA) carrier, the cell viability of carrier was 98%. In contrast, the cytotoxicity induced by 5-FU loaded NADES-poly(HEMA) carrier was 79%, which is higher activity of 5-FU in loaded carrier.

### 3.10 Cellular uptake studies

The cell uptake properties of as-synthesized 5-FU loaded NADES-poly(HEMA) carrier treated with HeLa cells and the results shown in Fig. 8. From the results, the cell uptake of 5-FU loaded NADES-poly(HEMA) was increased with increasing of days via more intense fluorescence representing a high accumulation of drug-loaded carrier in the HeLa cell lines. It is due to the 5-FU loaded NADES-poly(HEMA) carrier showed a gradual release of the 5-FU drug to the cell. Moreover, this carrier occurred in a sustained release manner and had the controlled release behavior. This could confirm that the 5-FU loaded NADES-poly(HEMA) carrier has penetrated the cell membrane and internalized into the cell nucleus [45].

## 4 Conclusion

In the current study, we developed bio-degradable 5-FU encapsulated NADES-poly(HEMA) carrier for sustainable anti-cancer drug delivery system. The 5-FU encapsulated NADES-poly(HEMA) carrier was successfully synthesized through polymerization of HEMA by the assistance of ChoCl:Xylitol (1:1) NADES. The structure, functionality, crystalline nature and morphology of the 5-FU encapsulated NADES-poly(HEMA) carrier were confirmed using NMR, FT-IR, XRD and SEM respectively. The sustainable cumulative drug releases from the 5-FU encapsulated NADES-poly(HEMA) carrier was observed and longer drug releasing nature up to 130 h was obtained. The NADES-poly(HEMA) showed no cytotoxicity effects against HeLa cells. The 5-FU encapsulated NADES-poly(HEMA) carrier showed higher cytotoxicity effects. Since NADES assisted polymeric carrier is a good platform for the delivering anti-cancer drug.

**Acknowledgements** M. Rajan is appreciative to the University Grants Commission (UGC), Government of India, for financial support under the plan of "UGC-MRP" (F. No. 43-187/2014 (SR) and UGC-BSR scheme (Ref: No. F. 30-21/20014 (BSR). M. Rajan thanks the University Grants Commission, New Delhi, for funds under the PURSE and UPE program.

### Compliance with ethical standards

**Conflict of interest** The authors declare that they have no conflict of interest.

## References

1. Tang B, Zhang H, Row KH (2015) Deep eutectic solvent-based microwave-assisted method for extraction of hydrophilic and hydrophobic components from radix salviae miltiorrhizae. J Sep Sci 38:1053–1064
2. Phadtare SB, Shankarling GS (2010) Halogenation reactions in biodegradable solvent: efficient bromination of substituted 1-aminoanthra-9,10-quinone in deep eutectic solvent (choline chloride:urea). Green Chem 12:458–462. https://doi.org/10.1039/B923589B
3. Francisco M, Bruinhorst A, Kroon MC (2012) New natural and renewable low transition temperature mixtures (LTTMs): screening as solvents for lignocellulosic biomass processing. Green Chem 14:2153–2157. https://doi.org/10.1039/C2GC35660K
4. Bica K, Rogers RD (2010) Confused ionic liquid ions—a "liquification" and dosage strategy for pharmaceutically active salts. Chem Commun 46:1215–1217
5. Carriazo D, Serrano MC, Gutiérrez MC, Ferrer ML, del Monte F (2012) Deep-eutectic solvents playing multiple roles in the synthesis of polymers and related materials. Chem Soc Rev 41:4996–5014
6. Aroso IM, Craveiro R, Rocha A, Dionísio M, Barreiros S, Reis RL, Paiva A, Duarte ARC (2015) Design of controlled release systems for THEDES—therapeutic deep eutectic solvents, using supercritical fluid technology. Int J Pharm 492:73–79
7. Tang B, Row K (2013) Application of deep eutectic solvents in the extraction and separation of target compounds from various samples. Monatsh Chem 144:1427–1454
8. Zhang Q, Vigier KO, Royer S, Jérôme F (2012) Deep eutectic solvents: syntheses, properties and applications. Chem Soc Rev 41:7108–7146
9. Choi SY, Rodríguez H, Mirjafari A, Gilpin DF, McGrath S, Malcolm KR, Tunney MM, Rogers RD, McNally T (2011) Dual functional ionic liquids as plasticisers and antimicrobial agents for medical polymers. Green Chem 13:1527–1535
10. Bangde PS, Ratnesh J, Prajakta D (2016) Alternative approach to synthesize methylated chitosan using deep eutectic solvents, biocatalyst and "green" methylating agents. ACS Sustain Chem Eng 4:3552–3557. https://doi.org/10.1021/acssuschemeng.6b00653
11. Dai YT, van Spronsen J, Witkamp GJ, Verpoorte R, Choi YH (2013) Natural deep eutectic solvents as new potential media for green technology. Anal Chim Acta 766:61–68
12. Wu YC, Wu P, Li YB, Liu TC, Zhang L, Zhou YH (2018) Natural deep eutectic solvents as new green solvents to extract anthraquinones from *Rheum palmatum* L. RSC Adv 8:15069
13. Bahadori L, Hashim MA, Manan NSA, Mjalli FS, AlNashef IMN, Brandon P, Chakrabarti MH (2016) Investigation of ammonium- and phosphonium-based deep eutectic solvents as electrolytes for a non-aqueous all-vanadium redox cell. J Electrochem Soc 163(5):A632–A638
14. Florindo C, Oliveira FS, Rebelo LPN, Fernandes AM, Marrucho IM (2014) Insights into the synthesis and properties of deep eutectic solvents based on cholinium chloride and carboxylic acids. ACS Sustain Chem Eng 2:2416–2425
15. Mukesh C, Upadhyay KK, Devkar RV, Chudasama NA, Raol GG, Prasad K (2016) Preparation of a noncytotoxic hemocompatible ion gel by self-polymerization of HEMA in a green deep eutectic solvent. Macromol Chem Phys 217:1899–1906. https://doi.org/10.1002/macp.201600122
16. Sanchez-Leija RJ, Pojman JA, Luna-Barcenas G, Mota-Morales JD (2014) Controlled release of lidocaine hydrochloride from polymerized drug-based deep-eutectic solvents. J Mater Chem B 2:7495
17. Serrano MC, Gutiérrez MC, Jiménez R, Ferrer ML, del Monte F (2012) Synthesis of novel lidocaine-releasing poly(diol-co-citrate) elastomers by using deep eutectic solvents. Chem Commun 48:579–581
18. Hou C, Lin S, Liu F, Hu J, Zhang G, Liu G, Tu Y, Zou H, Luo H (2014) Synthesis of poly(2-hydroxyethyl methacrylate) end-capped with asymmetric functional groups via atom transfer radical polymerization. New J Chem 38:2538
19. Smith TJ, Mathias LJ (2002) Synthesis and characterization of polymeric materials derived from multifunctional alkyl a-hydroxymethylacrylates. Biomacromolecules 3:1392–1399
20. Liu J, Lu JF, Kan J, Jin CH (2013) Synthesis of chitosan-gallic acid conjugate: structure characterization and in vitro anti-diabetic potential. Int J Biol Macromol 62:321–329
21. Zuber M, Tabasum S, Jamil T, Shahid M, Hussain R, Feras KS, Bhatti KP (2014) Biocompatibility and microscopic evaluation of polyurethane–poly(methyl methacrylate)–titnanium dioxide based composites for dental applications. J Appl Polym Sci 131(3):1–9
22. Shi M, Kretlow JD, Spicer PP, Tabata Y, Demian N, Wong ME, Kasper FK, Mikos AG (2011) Antibiotic-releasing porous polymethylmethacrylate/gelatin/antibiotic constructs for craniofacial tissue engineering. J Control Release 152(1):196–205
23. Serrano MC, Carbajal L, Ameer GA (2011) Novel biodegradable shape-memory elastomers with drug-releasing capabilities. Adv Mater 23(19):2211–2215

24. Nicolas J (2016) Drug-initiated synthesis of polymer prodrugs: combining simplicity and efficacy in drug delivery. Chem Mater 28:1591–1606
25. Singh B, Dhiman A, Kumar A (2016) Slow release of ciprofloxacin from β-cyclodextrin containing drug delivery system through network formation and supramolecular interactions. Int J Biol Macromol 92:390–400
26. Dash TK, Konkimalla VB (2012) Polymeric modification and its implication in drug delivery: poly-ε-caprolactone (PCL) as a model polymer. Mol Pharm. https://doi.org/10.1021/mp300 1952
27. Stott PW, Williams AC, Barry BW (1998) Transdermal delivery from eutectic systems: enhanced permeation of a model drug, ibuprofen. J Control Release 50:297–308
28. Abbott AP, Boothby D, Capper G, Davies DL, Rasheed RK (2004) Deep eutectic solvents formed between choline chloride and carboxylic acids: versatile alternatives to ionic liquids. J Am Chem Soc 126:9142–9147
29. Kumar SSD, Mahadevan S, Vijayaraghavan R, BaranMandal A, MacFarlane DR (2014) Curcumin loaded poly(2-hydroxyethyl methacrylate) nanoparticles from gelled ionic liquid—in vitro cytotoxicity and anti-cancer activity in SKOV-3 cells. Eur J Pharm Sci 51:34–44
30. Pradeepkumar P, Govindaraj D, Jeyaraj M, Munusamyc MA, Rajan M (2017) Assembling of multifunctional latex-based hybrid nanocarriers from *Calotropis gigantea* for sustained (doxorubicin) DOX releases. Biomed Pharmacother 87:461–470
31. Pradeepkumar P, Elgorban AM, Bahkali AH, Rajan M (2018) Natural solvent-assisted synthesis of amphiphilic co-polymeric nanomicelle for prolonged release of camptothecin delivery. New J Chem. https://doi.org/10.1039/c8nj00901e
32. Gomathi T, Govindarajan C, Rose HR, Sudha PN, Imran PKM, Venkatesan J, Kim SK (2014) Studies on drug–polymer interaction, in vitro release and cytotoxicity from chitosan particles excipient. Int J Pharm 468:214–222
33. Nakamura H, Koziolová E, Chytil P, Tsukigawa K, Fang J, Haratake M, Ulbrich K, Etrych T, Maeda H (2016) Pronounced cellular uptake of pirarubicin versus that of other anthracyclines: comparison of HPMA copolymer conjugates of pirarubicin and doxorubicin. Mol Pharm 13(12):4106–4115
34. Mbous YP, Hayyan M, Hayyan A, Wong WF, Hashim MA, Looi CY (2016) Applications of deep eutectic solvents in biotechnology and bioengineering-Promises and challenges. Biotechnol Adv 35(2):105–134
35. Pérez-García MG, Gutiérrez MC, Mota-Morales JD, Luna-Bárcenas G, Del Monte F (2016) Synthesis of biodegradable macroporouspoly(L-lactide)/poly(ε-caprolactone) blend using oil-in-eutectic-mixture high internal phase emulsions as template. ACS Appl Mater Interfaces 8(26):16939–16949
36. Mota-Morales JD, Gutiérrez MC, Sanchez IC, Luna-Bárcenas G, del Monte F (2011) Frontal polymerizations carried out in deep-eutectic mixtures providing both the monomers and the polymerization medium. Chem Commun 47:5328–5330
37. Yadav A, Pandey S (2014) Densities and viscosities of (choline chloride + urea) deep eutectic solvent and its aqueous mixtures in the temperature range 293.15 K to 363.15 K. J Chem Eng Data 59:2221–2229
38. Zaid HFM, Chong FK, Mutalib MIA (2017) Extractive deep desulfurization of diesel using choline chloride-glyceroleutectic-based ionic liquid as a green solvent. Fuel 192:10–17
39. Shinar H, Battistel MD, Mandler M, Lichaa F, Freedberg DI (2014) chemical exchange saturation transfer NMR of oligo- and polysialic acids and the assignment of their hydroxyl groups using selective- and HSQC-TOCSY. Carbohydr Res 389:165–173
40. Rajan M, Murugan M, Ponnamma D, Sadasivuni K, Munusamy MA (2016) Poly-carboxylic acids functionalized chitosan nanocarriers for controlled and targeted anti-cancer drug delivery. Biomed Pharmacother 83:201–211
41. Gheybi H, Entezami AA (2013) Nanosized micelles self-assembled from amphiphilicpoly(citric acid)–poly(e-caprolactone)–poly(citric acid) copolymers. Polym Bull 70:1875–1894
42. Zhao H, Gary AB, Shaletha H (2011) Protease activation in glycerol-based deep eutectic solvents. J Mol Catal B Enzym 72:163–167
43. Rajan M, Raj V, Al-Arfaj AA, Murugan AM (2013) Hyaluronidase enzyme core-5-fluorouracil-loaded chitosan-PEG-gelatin polymer nanocomposites as targeted and controlled drug delivery vehicles. Int J Pharm 453:514–522
44. Mao J, Li Y, Wu T, Yuan C, Zeng B, Xu Y, Dai L (2016) Layer-by-layer polyelectrolyte assisted growth of 2D ultrathin $MoS_2$ nanosheets on various 1D carbons for superior Li-storage. ACS Appl Mater Interfaces 8:17109–17117
45. Liu X, Wei W, Huang S, Lin SS, Zhang X, Zhang C, Du Y, Ma G, Li M, Mann S, Ma D (2013) Bio-inspired protein–gold nanoconstruct with core–void–shell structure: beyond a chemo drug carrier. J Mater Chem B 1:3136